JOC The Journal of Organic Chemistry

Article

pubs.acs.org/joc

Fluorescent Molecular Rotors of Organoboron Compounds from Schiff Bases: Synthesis, Viscosity, Reversible Thermochromism, Cytotoxicity, and Bioimaging Cells

Marisol Ibarra-Rodríguez,[†] Blanca M. Muñoz-Flores,[†] H. V. Rasika Dias,[‡] Mario Sánchez,[§] Alberto Gomez-Treviño,[†] Rosa Santillan,[∥] Norberto Farfán,[⊥] and Víctor M. Jiménez-Pérez*[,†]

[†]Facultad de Ciencias Químicas, Ciudad Universitaria, Universidad Autónoma de Nuevo León, 66451 San Nicolás de los Garza, Nuevo León Mexico

[‡]Department of Chemistry and Biochemistry, The University of Texas at Arlington, Arlington, Texas 76019-0065, United States

[§]Centro de Investigación en Materiales Avanzados, S.C., Alianza Norte 202, PIIT, Carretera Monterrey-Aeropuerto Km 10, CP 66628, Apodaca, Nuevo León Mexico

[∥]Departamento de Química, Centro de Investigación y de Estudios Avanzados del IPN, A.P. 14-740, CP 07000 San Pedro Zacatenco, DF, Mexico

[⊥]Facultad de Química, Departamento de Química Orgánica, Universidad Nacional Autónoma de México, Ciudad Universitaria, 04510 Mexico City, Mexico

Supporting Information

ABSTRACT: We report the design, synthesis, and characterization of two new fluorescent molecular rotors of boron derived from Schiff bases: (2,4,8,10-tetra-*tert*-butyl-6-phenyldibenzo[*d*,*h*][1,3,6,2]-dioxazaboronine (**3**) and 1,4-bis(2,4,8,10-tetra-*tert*-butyldibenzo[*d*,*h*]-[1,3,6,2]dioxazaboronin-6-yl)benzene (**4**), as well as the free ligand 2-[[(3,5-di-*tert*-butyl-2-hydroxyphenyl)imino]methyl]-4,6-di-*tert*-butyl-phenol **1**. All compounds were fully characterized by NMR (^{1}H, ^{11}B, and ^{13}C), IR, UV/vis, fluorescence spectroscopy, and high-resolution mass spectrometry. The crystal structures of **3** and **4** showed tetracoordinated boron atoms with semiplanar skeleton ligands. The free rotation of the fluorescent molecular rotor, only observed in the binuclear compound, was decreased with increasing viscosity, while the quantum yield was increased. Interestingly, the property of reversible thermochromism was found in organoboron **4** in the solid state. DFT calculations to determine the both complexes have free rotation around the CPh−B1 bond. The boron compounds **3** and **4** have shown low cytotoxicity activity in cell line A-431 and low green staining in cells.

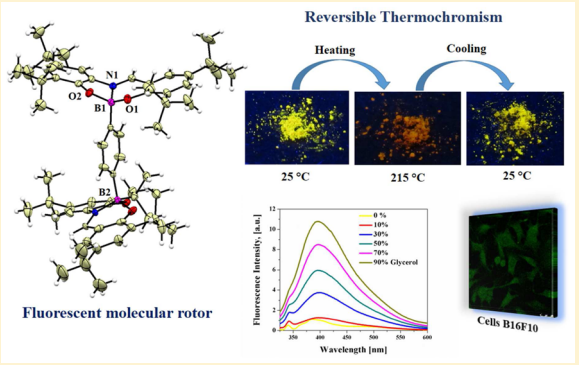

1. INTRODUCTION

Fluorescent molecular rotors (FMRs) with viscosity-sensitive quantum yields[1] have received tremendous attention due to their potential application in the detection of biomolecular interactions,[2] polymerization processes,[3] and microviscosity.[4] Viscosity plays an important role in living organisms, and fluorescence imaging with molecular rotors is a technique that helps viscosity studies on a cellular scale.[5] Other potential applications of rotors involve their use as sensors to measure viscosity in biofluid.[6] Organoboron compounds are interesting in this regard. Different types of luminescent rotors of boron are known, such as BODIPYs, chalcone derivatives, and boronates (Chart 1, **I**–**X**).[7] The BODIPYs are the most widely studied group. Benniston and co-workers reported that the compound **I** can be used to record how certain fluids respond to applied pressures and changes of viscosity in the medium. The mechanism involves the gyration of the mesophenylene ring and accompanying distortion of the dipyrromethene framework.[8] In another example, Shiraishi et al. reported that the compound **V** serves as a fluorescent thermometer in water and the fluorescence increases in the copolymer due to increase in viscosity,[9] with behavior similar to that reported in compound **II** in which the fluorescence intensity increases with the restricted rotation of the phenyl group in a medium of high viscosity. This property can be exploited as a practical and versatile tool to measure microviscosity.[10] Other groups have investigated chalcone derivatives. Klymchenko and co-workers reported that compound **VII** shows solvatochromic property and acts as a viscosity-sensitive molecular rotor.[11] The organoboron compounds show low cytotoxicity.[12] The synthetic methods, however, involve several steps and require specific conditions

Received: November 23, 2016
Published: January 30, 2017

© 2017 American Chemical Society

DOI: 10.1021/acs.joc.6b02802
J. Org. Chem. 2017, 82, 2375−2385

Chart 1. Luminescent Molecular Rotors of Organoboron Compounds

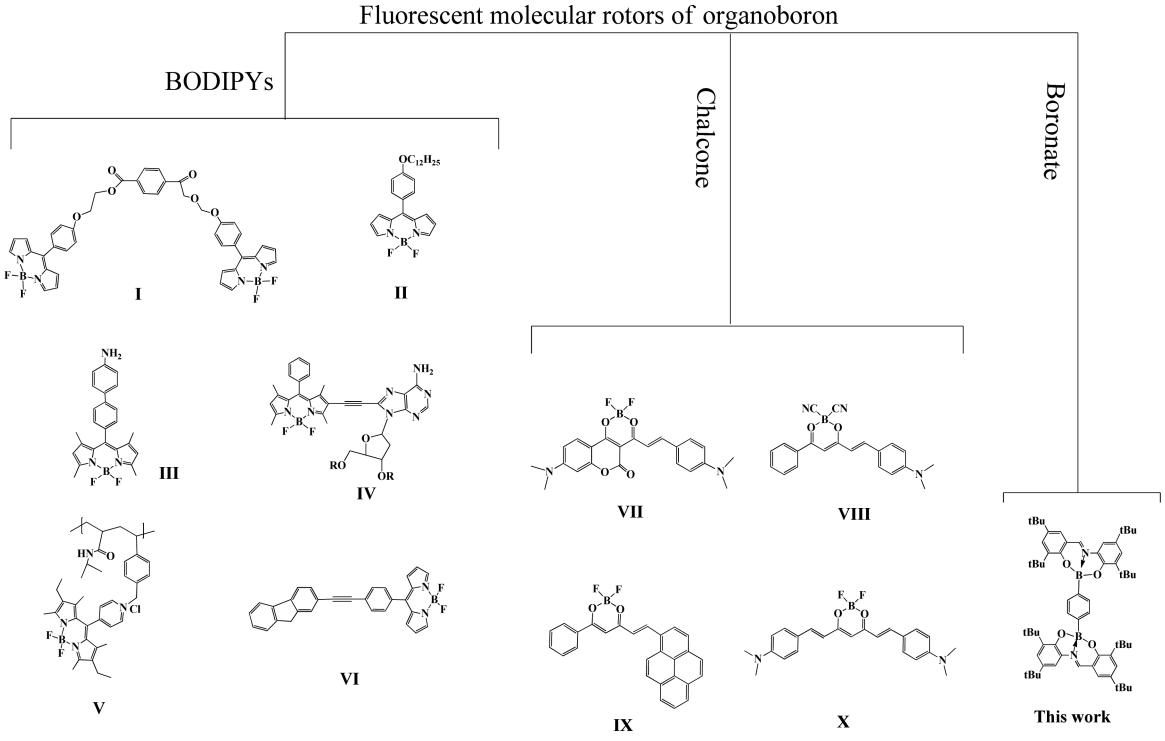

Scheme 1. Synthesis of Ligand 2 and Organoboron Compounds 3 and 4

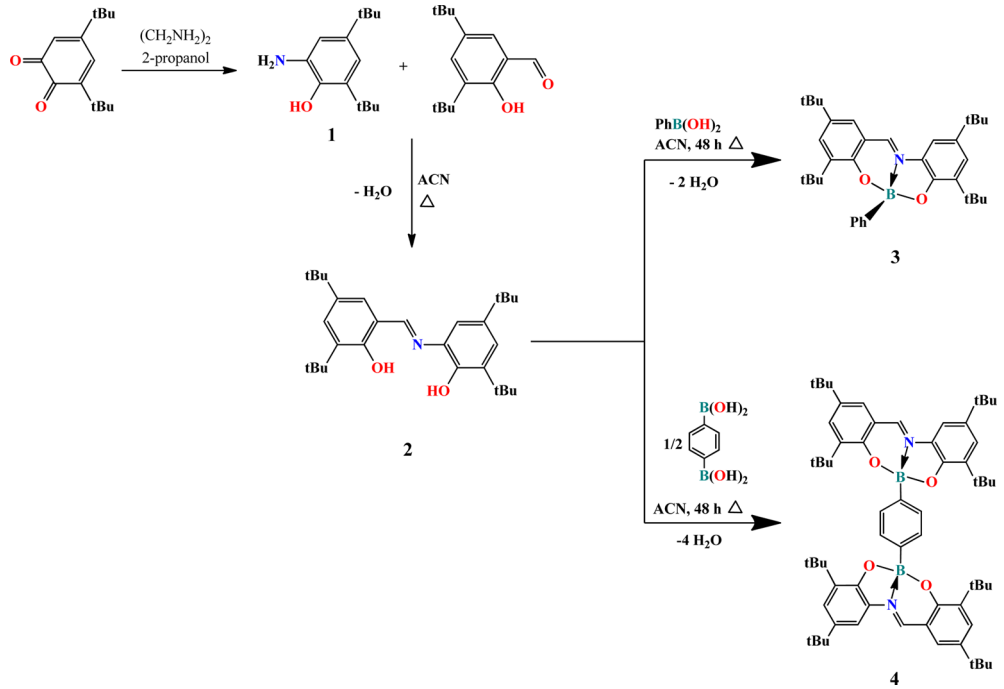

as anhydrous atmospheres as evident in the BODIPY chemistry.[13]

Fluorescent sensors have received attention because they have advantages in terms of sensitivity, selectivity, and the easy detection of the fluorescence changes of the systems.[14] Previously, transition-metal complexes have been reported that exhibit the property of change in color at different temperatures. This phenomenon is called luminescent thermochromism and represents an important area of solid-state chemistry.[15] The thermochromic materials are potentially useful in thermometers, as temperature sensors, and in the development of warning signals and optoelectronic display devices.[16] An interesting study of the thermochromism properties of copper pyrazolates, promising compounds for sensor applications, was reported by Dias and co-workers.[17] Other examples involve copper iodine clusters that show reversible luminescence thermochromism with intense orange emissions[18] and $Au^{1}-Cu^{1}$ phosphine complexes that exhibit reversible emission change from yellow

DOI: 10.1021/acs.joc.6b02802
J. Org. Chem. 2017, 82, 2375−2385

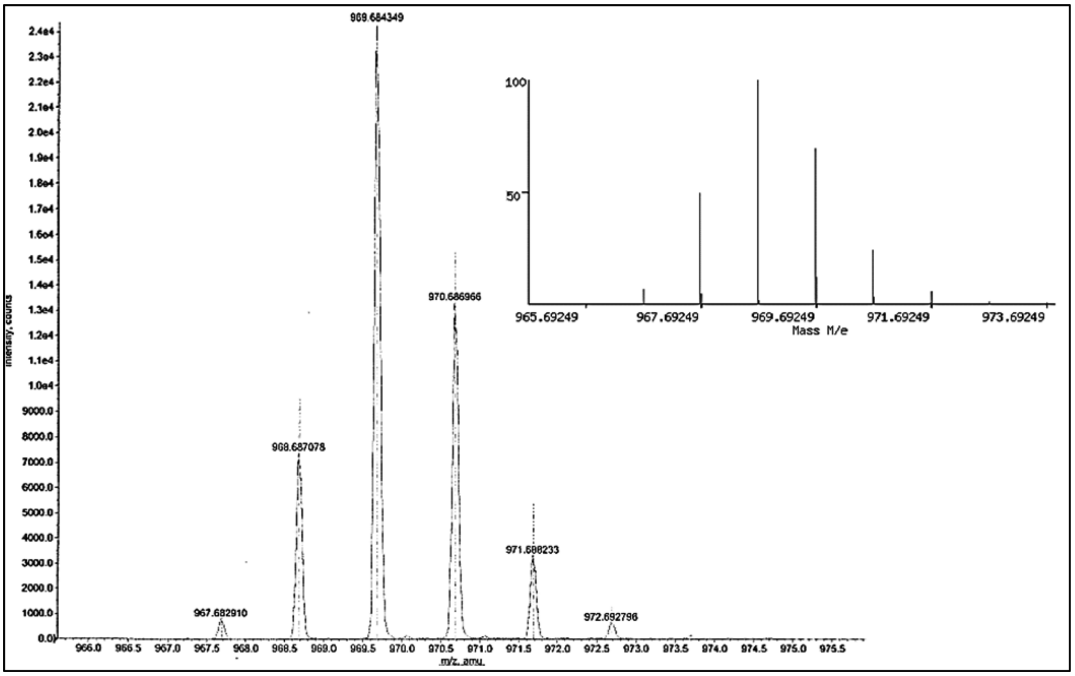

Figure 1. Comparison of theorical and experimental isotopic distributions of spectra of the $[M + H]^+$ of compound **4**; the spectrum clearly indicates the presence of two boron atoms.

to green.[19] Another group has investigated triarylboron compounds and their utility as excellent real-time and reversible temperature indicators with a concentration-independent feature.[20]

Recently, our research group reported the synthesis of a series of novel luminescent boron derivatives of tridentate ligands with good solubility in polar solvents.[21] In this work, we describe the synthesis of luminescent boron derivatives of Schiff bases that act as molecular rotors and their use as cell markers.

2. RESULTS AND DISCUSSION

2.1. Synthesis. Previously, similar binuclear organoboron compounds derived from tridentated ligands have been synthesized and characterized by common spectroscopic and spectrometric methods. However, due to the low solubility in some organic solvents, it was not possible to isolate the crystal structures or complete the solution characterization.[22] In order to improve the solubility, we have designed a new Schiff base ligand **2** which was prepared by condensation reaction of 3,5-di-*tert*-butyl-2-hydroxybenzaldehyde with 3,5-di-*tert*-butyl-6-hydroxyaniline (**1**), and the boron compounds **3** and **4** were obtained by condensation of phenylboronic acid and diacid with the ligand under reflux in acetonitrile (Scheme 1), respectively. The resulting organoboron complexes are soluble in several organic solvents; both complexes were stable in the solid state. The compounds were fully characterized by NMR (^{1}H, ^{11}B, and ^{13}C) and IR spectroscopy, and mass spectrometry. The complexes **3** and **4** were characterized by single-crystal X-ray diffraction (vide infra).

2.2. Solution and Solid Structures. The existence of the N → B coordination bond was evidenced by ^{11}B NMR spectra for compound **3** with one broad signal of 7.88 ppm indicative of a tetracoordinated boron atom.[23] In the ^{13}C spectra of boron for complexes, the signals for C7 were shifted to low frequencies (151.73, 147.14 ppm) with respect to the ligand (165.45 ppm) owing to coordination to boron, and the imine proton was observed at (**3**) 8.78 ppm, (**4**) 8.13 ppm.[24] IR spectral analysis showed that the C═N stretching vibration bands for **3** and **4** were shifted to lower wavenumbers in comparison with the ligand.[25] The mass spectra of boron derivatives showed the base peak corresponding to the molecular ion peak and, for complex **4**, the first fragmentation of the complex by removing the methyl substituent groups *tert*-butyl and the fragment of ligand coordinated to a boron atom 446.32 *m*/*z* (6.17%); the isotopic distribution of parent ions in the spectra demonstrated the presence of two atoms of boron in the organoboron **4**. The comparison of predicted theoretical and experimental isotopic distributions of spectra for compound **4** is given in Figure 1.

2.3. X-ray Structure. Complexes **3** and **4** crystallized from slow evaporation of ACN and THF/acetone. Suitable single

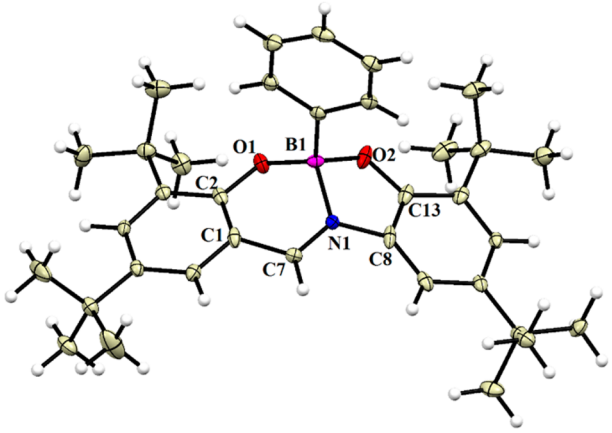

Figure 2. View of the structure of the **3**. Ellipsoids are drawn at the 30% probability level. Distances: B(1)−O(1) 1.4536 (18), B(1)−O(2) 1.4774(19), B(1)−N(1) 1.596(2), B(1)−C(14) 1.609(2) Å. Bond angles: O(2)−B(1)−C(14) 111.61 (11), O(1)−B(1)−C(14) 113.77 (11), O(2)−B(1)−N(1) 95.13(11), O(2)−B(1)−O(1) 112.75(11), N(1)−B(1)−C(14) 110.81(11), O(1)−B(1)−N(1) 111.33(12)°.

DOI: 10.1021/acs.joc.6b02802
J. Org. Chem. 2017, 82, 2375−2385

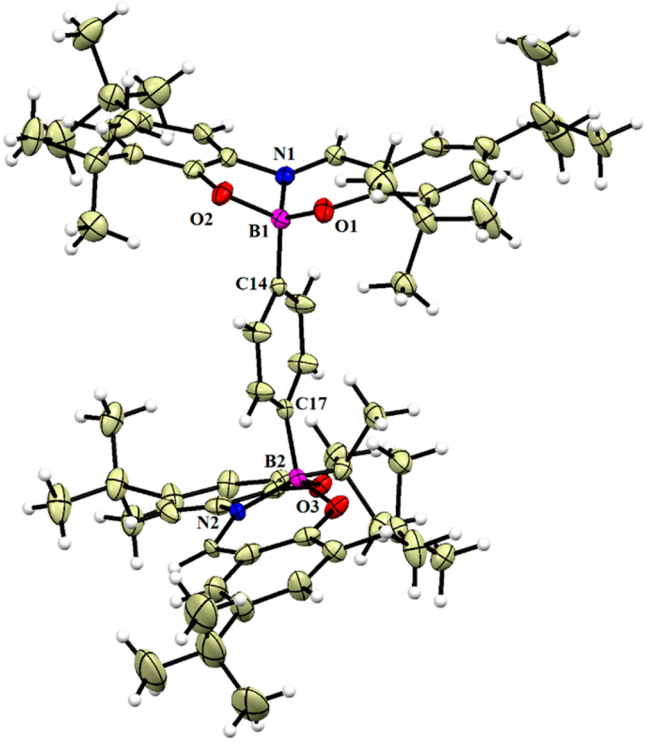

Figure 3. View of the structure of the **4**. Ellipsoids are drawn at the 30% probability level. Distances: B(1)−C(14) 1.591(3), B(1)−O(1) 1.451(3), B(1)−O(2) 1.455(3), B(1)−N(1) 1.587(6), B(2)−C(17) 1.593(3), B(2)−O(4) 1.471 (3), B(2)−N(2) 1.563(6), B(2)−O(3) 1.460(3) Å. Bond angles: O(2)−B(1)−C(14) 114.83(19), O(1)−B(1)−C(14) 112.56(19), O(2)−B(1)−N(1) 91.4(2), O(1)−B(1)−N(1) 90.8(2), O(2)−B(1)−O(1) 110.57(18), N(1)−B(1)−C(14) 110.0(2), O(4)−B(2)−C(17) 113.03(18), O(3)−B(2)−C(17) 111.89(18), O(3)−B(2)−N(2) 90.8(3), N(2)−B(2)−O(4) 91.9(2), O(4)−B(2)−O(3) 111.45(18), C(17)−B(2)−N(2) 114.5(2)°.

crystals for X-ray analysis were obtained for **3** and **4**, and their molecular structures are shown in Figures 2 and 3, while data collection and refinement parameters and bond lengths and angles are available in Tables S1 and S2. Both complexes crystallized in $P2_1/n$ space group and are monoclinic. Complex **3** crystallized as an orange block, and **4** crystallized as an orange diamond with molecules of solvent acetone.

The crystal structures of **3** and **4** display tetracoordinated boron atoms with distorted tetrahedral geometry and the formation of two fused heterocycles of five and six members. The B−O bond distances [**3** (1.454−1.477 Å), **4** (1.451−1.471 Å)] are characteristic for tetracoordinated boron complexes and are comparable to the previously reported values.[26] The B−N bond lengths [**3** (1.596 Å), **4** (1.560−1.587 Å)] suggest strong coordination of the nitrogen atoms with boron atoms because are they are less than the estimated covalent N−B distance; this is confirmed by the tetrahedral character of 89.8 and 90.0−91.7% for each molecule.[27] The distortion of the tetrahedral geometry causes the boron atom to lie outside the plane from the salicylidene ring (**3**: plane: N1−C1−C2−C3−O1, θ = 0.519 Å, **4**: plane: N1−C1−C2−C3−O1, θ = 0.407 Å). Crystal structures of **3** and **4** show various close intermolecular [**3** (H7−C15, 2.80 Å), **4** (imine H−O other molecule, 2.291, 2.514 Å); (imine H−acetone oxygen, 2.222 Å); (H of acetone with ring (centroids 1 and 2, see Figure S18), 2.921 and 2.771 Å)] and intramolecular interactions [**3** (H19−O1, 2.603 Å), (H15−O2, 2.758 Å); **4** (H15−N1, 2.515), (H19−O1, 2.975), (H16−O3, 2.510), see Figure 4].

2.4. Photophysical Characterization. The optical properties of compounds were obtained in THF, chloroform, and methanol (Table 1). The absorption and emission spectra for **3** and **4** are shown in Figure 5. For compounds **3** and **4**, the absorption bands show two λ_{max} in 319 and 460 nm, which can be ascribed to the HOMO−LUMO electronic transition; the molar extinction coefficients (ε) of **3** and **4** were in the range of 4000−21000 M^{-1} cm^{-1} in different solvents. The optical band gaps (eV) are characteristic of semiconductor materials. The fluorescence spectrum of complexes **3** and **4** show emissions around 520 nm in THF and $CHCl_3$. However, it is interesting to observe that both compounds showed one emission at 386 nm in

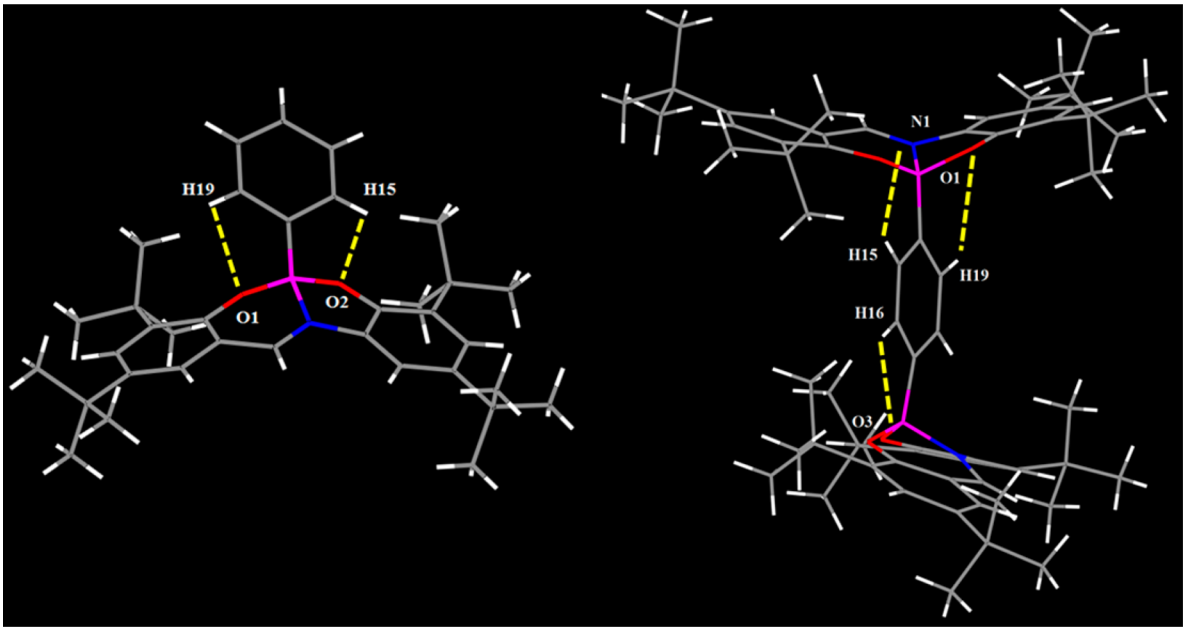

Figure 4. Intramolecular interactions of **3** and **4** [**3** (H19−O1, 2.603), (H15−O2, 2.758); **4** (H15−N1, 2.515), (H19−O1, 2.975), (H16−O3, 2.510)].

DOI: 10.1021/acs.joc.6b02802
J. Org. Chem. 2017, 82, 2375−2385

Table 1. Photophysical Data of Compounds 3 and 4

compd	solvent	λ_{abs} (nm)	$\varepsilon \times 10^4$ (M^{-1} cm^{-1})	E_g (eV)	λ_{em} (nm)	dyn viscosity (mPa·s)	Φ_F (%)
3	THF	319, 455	1.4	2.41	514	0.55	0.002
	chloroform	324, 460	1.9	2.35	529	0.55	0.09
	methanol	320, 447	0.5	2.41	387	0.60	0.68
4	THF	319, 455	2.1	2.41	512	0.55	0.10
	chloroform	322, 461	1.2	2.33	523	0.55	1.69
	methanol	319, 450	0.4	2.41	385	0.60	0.56

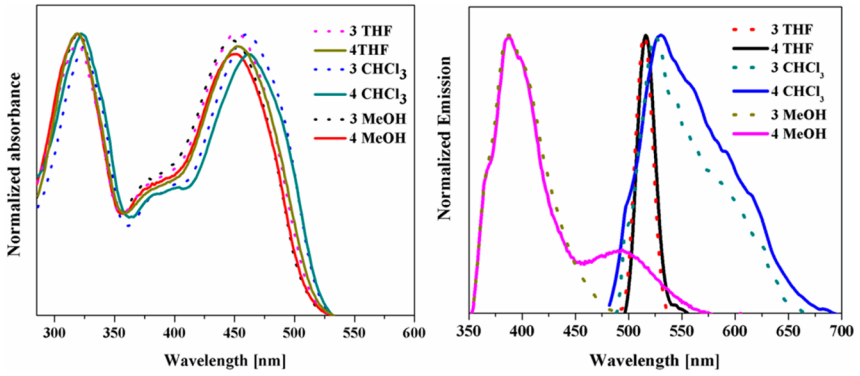

Figure 5. Absorption and emission spectrum of compounds **3** and **4** in THF, $CHCl_3$, and MeOH.

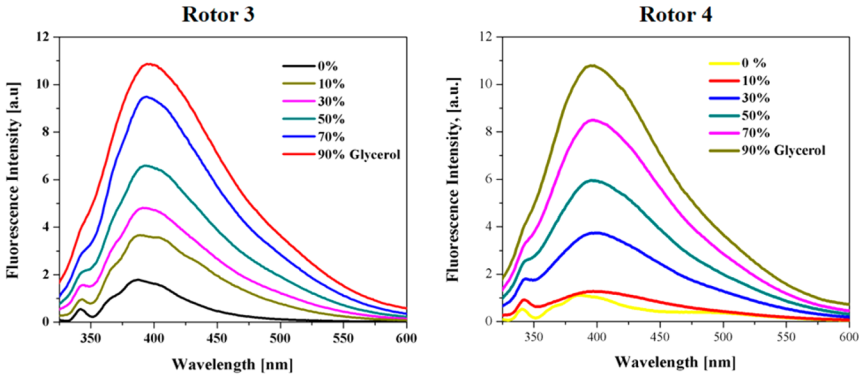

Figure 6. Fluorescence spectra of compounds **3** and **4** in binary mixtures of methanol and glycerol in different ratios.

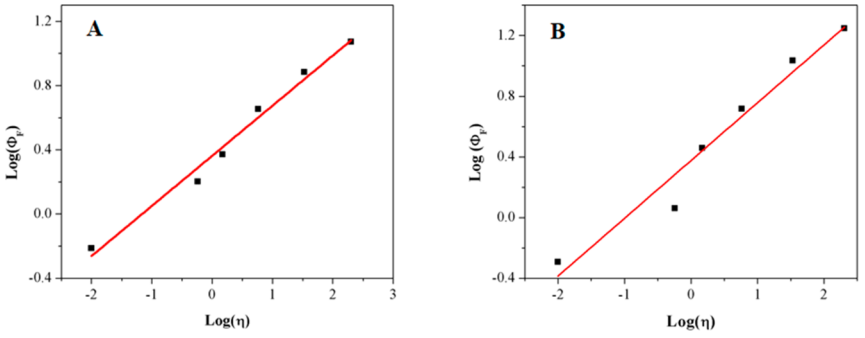

Figure 7. Correlation of the fluorescence quantum yield (Φ_F) of organoboron **3** (A) and **4** (B) with values for the viscosity of the medium r^2 (goodness of fit) of 0.98−0.95.

methanol. This behavior is due to the difference of solvent dynamic viscosities (Table 1) as has been reported by molecular rotors.[28]

Fluorescence measurements of mononuclear **3** and dinuclear **4** in methanol/glycerol mixtures of different viscosities (% of glycerol) show that the fluorescence quantum yield increases with increasing solvent viscosity (Figure 7) according to the Föster−Hoffman equation.[29] The observed increase in fluorescence intensity is consistent with the restricted rotation of the phenyl (bonded to the boron atom see Figure 6) in the medium of high viscosity and dissipated energy by intramolecular rotation, and the photoactivated molecule may relax by a nonradiative decay processes. The emission intensity increased more for compound **4** with medium viscosity (see Table 2)

DOI: 10.1021/acs.joc.6b02802
J. Org. Chem. 2017, 82, 2375−2385

because it has two points of rotation in the structure of the molecule; in the literature, we find this behavior for ligands and complexes.[30]

Table 2. Spectroscopic Properties of Compounds 3 and 4 in Binary Mixtures of Methanol and Glycerol[a]

glycerol fraction (v/v)	compd 3			compd 4		
	λ_{abs} (nm)	λ_{em} (nm)	Φ_F (%)	λ_{abs} (nm)	λ_{em} (nm)	Φ_F (%)
0	447	387	0.61	448	387	0.51
10	449	388	1.59	446	398	1.15
30	449	391	2.35	453	397	2.87
50	450	392	4.50	455	397	5.21
70	451	394	7.64	454	397	10.81
90	463	395	11.82	460	395	17.63

[a]Methanol/glycerol mixture; λ_{abs} and λ_{em} are absorption and emission maxima; Φ_F is the fluorescence quantum yield.

2.5. Reversible Thermochromism. The organoboron **4** shows the ability to behave as a thermochromic material; the luminescence property was modified when the complex was exposed to different temperatures. During heating at 215 °C, the color changed from yellow to orange and the luminescence intensity decreased under UV radiation to the naked eye, but after cooling at room temperature the property returned (Figure 8A–C).[31] The thermochromic property of **4** was determined by

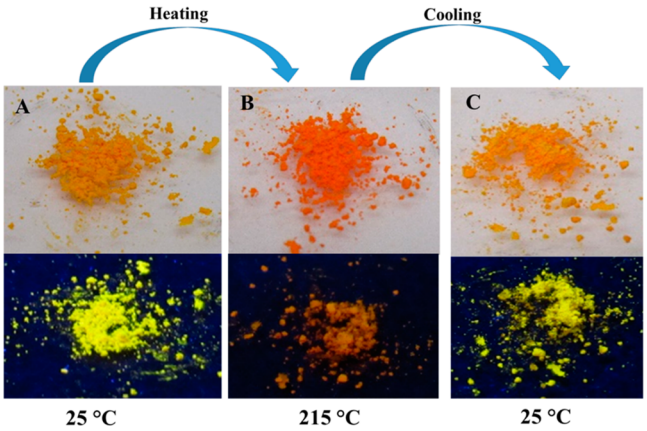

Figure 8. Fluorescence image of compound **4**: (A) under vis and UV light at 25 °C; (B) under vis and UV light at 215 °C; (C) after cooling under vis and UV light at 25 °C.

luminescence spectroscopy in the solid state (Figure 9). However, when compound **4** was ground for 2 min on a mortar the luminescence property was lost (see Figure S19), similar to that reported by Seki et al.[32]

2.6. DFT Calculations. In order to explain the molecular behavior for complexes **3** and **4**, we performed a theoretical study using the density functional theory (DFT, B3LYP) in combination with the 6-31G(d,p) basis set. All of the structures were characterized by calculating their frequencies. Our results suggest that structure **4** with a *trans* conformation is more stable than the *cis* configuration by only 1.38 kcal/mol; the explanation for this is that the structure with the *cis* conformation has more steric hindrance (Figure 10). Interestingly, the structure that has crystallized and characterized by X-ray has no symmetry because one of the two ligands is displaced by 60°. This behavior could be

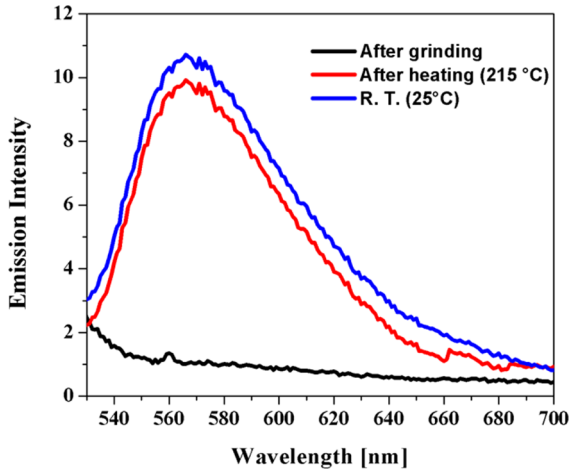

Figure 9. Luminescence spectra of compound **4** at room temperature after heating and after grinding.

attributed to acetone trapped into the crystal lattice (see Figure S18).

To better understand the process of rotation of the aromatic ring for complex **4**, we have followed two strategies; the first was to rotate only one ligand, and the second was to rotate only the aromatic ring, keeping the two ligands fixed, and both rotating processes were performed every 30° along the potential energy surface (Figure 10). The results of these calculations can be observed in Figure 11. The energy barrier value for complex **4** to rotate the aromatic ring is higher because of steric effects generated by the *tert*-butyl groups. However, when only one ligand is rotated the relative energy value (energy barrier) is smaller.

On the other hand, the rotation of the phenyl group in the complex **3** was also studied. Complex **3** shows an energy barrier value of 6.26 kcal/mol by rotating the CPh–B1 bond every 30°; with these results, we can mention that both complexes present free rotation.

In addition, we have also calculated the UV–vis spectra in both complexes **3** and **4**. The experimental (460 and 461 nm, respectively) absorption values are very similar to those calculated (463 and 465 nm, respectively).When we explored the rotational energy barrier of the rotational ligand and phenyl groups, we found that for the complex **4** up to 120° the degree of absorption (482 nm) is slightly higher than that found in the global minimum (465 nm). This difference is because the structure **4** (120°) involves $\pi-\pi$ transitions (see Figure S1). It is important to mention that the B3LYP method tends to slightly modify the energies of the rotation barriers,[33] compared to other functional ones. We have used B3LYP because of its wide use in organic molecules.

Molecular orbitals and their energies for the complexes **3** and **4** are shown in Figure 12 The electron density is mostly located on the ligands of both complexes and the electronic transitions, which mainly involve the HOMO−1 → LUMO and HOMO → LUMO+1 frontier orbitals for the binuclear compound that corresponds to the $\pi-\pi^*$ transitions (Tables S4–6).

2.7. Cytotoxicity Activity and Cell Images. In vitro cytotoxicity activity of organoboron **3** and **4** were evaluated on epidermoid carcinoma cell line A-431 in different concentrations (from 20 to 1 μg/mL) for 24 h. As DMSO was the solvent used for the compounds, its toxicity was analyzed. The viability of the cells shows lower toxicity for organoboron **3** and **4** in all tested

DOI: 10.1021/acs.joc.6b02802
J. Org. Chem. 2017, 82, 2375–2385

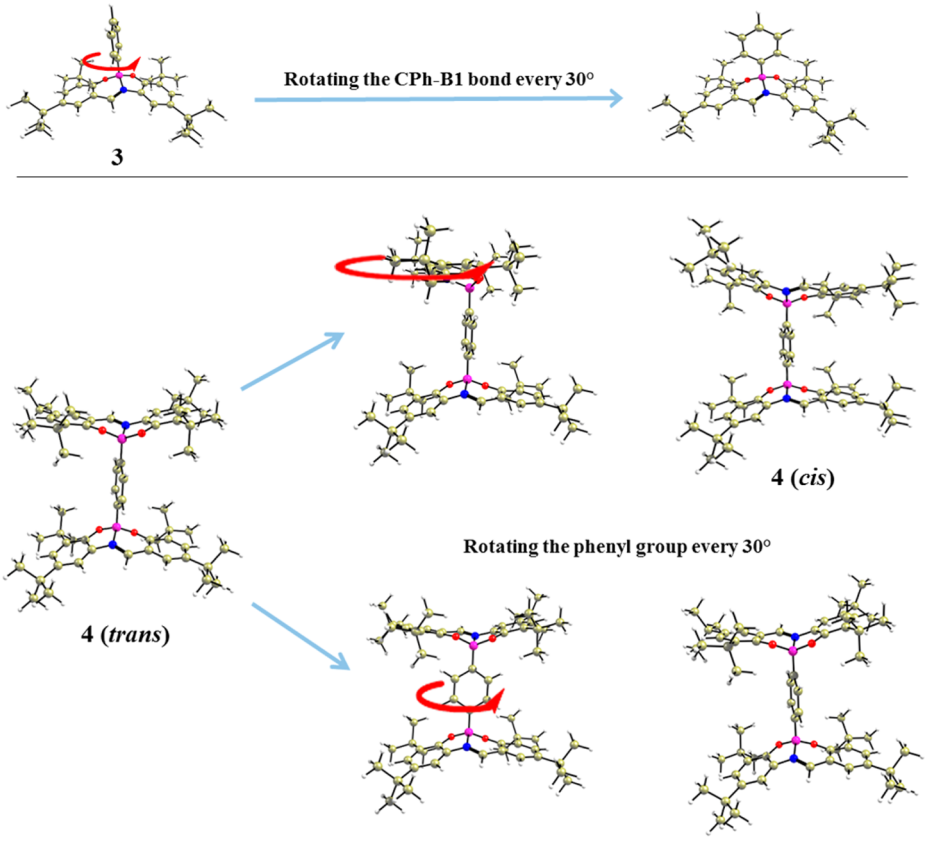

Figure 10. Rotation of ligand and phenyl groups in complexes **3** and **4**.

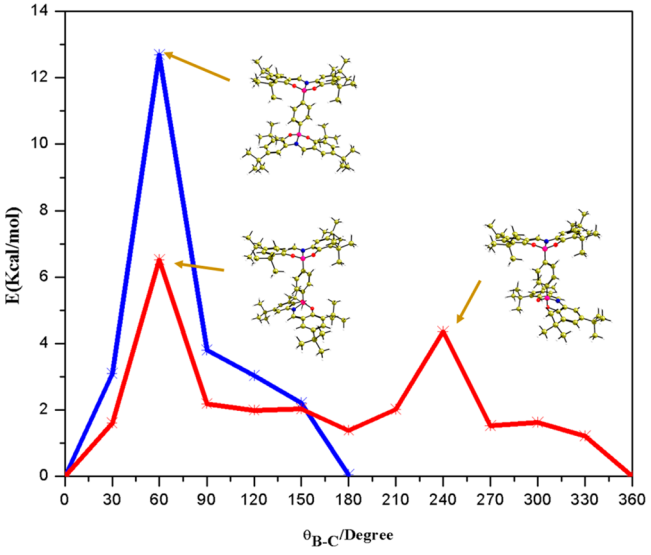

Figure 11. Rotation barrier energies for complex **4**. Blue line belongs to the rotation of the phenyl group, while the red line belongs to the rotation of the CPh−B1 bond.

concentrations (20−38 μM, 20 μg/mL highest concentration); see Figure 13. This behavior has already been reported for molecules having low cytotoxicity to 10 μM.[34] The dinuclear compound shows lower cytotoxicity and tends to be less soluble and less penetrating for the compound in the cell.

To determine the capacity of the organoboron compounds to produce fluorescent stain on cells, A431 and B16F10 cells were treated with 10 μg/mL for 2 h and then analyzed by confocal laser microscopy; cells treated with the organoboron compounds **3** and **4** presented a low green staining, due to poor solubility of the compounds in the polar solvents, and fluorescence was observed from the cytoplasm in both cases (Figure 14).

3. CONCLUSIONS

In summary, we describe the synthesis, characterization in solution and solid state, and X-ray structure of two new fluorescent organoboron compounds. The binuclear compound shows that the fluorescence quantum yield increases strongly with increasing solvent viscosity, and due to the rotor molecular property, it was corroborated through B3LYP that organoboron has the property of reversible thermochromism. Both fluorescent organoboron compounds have shown low cytotoxicity, which is good for potential medical applications but has a poor capacity for staining cells. We are working to improve the hydrophilicity of fluorescent molecular rotors of organoboron compounds. The binuclear molecular rotor showed reversible thermochromism as well as visco- and solvoluminescene. To the best of our knowledge, this is the first example which showed this multiresponse.

4. EXPERIMENTAL SECTION

4.1. Material and Equipment. All starting materials and solvents were used without further purification. Compound **1** was synthesized as previously reported.[35] Melting points were performed on an Mel-Temp apparatus and are uncorrected. High-resolution mass spectra were obtained by LC/MSD TOF with APCI as ionization source. Infrared spectra were recorded using a 27 FT-IR spectrophotometer equipped

DOI: 10.1021/acs.joc.6b02802
J. Org. Chem. 2017, 82, 2375−2385

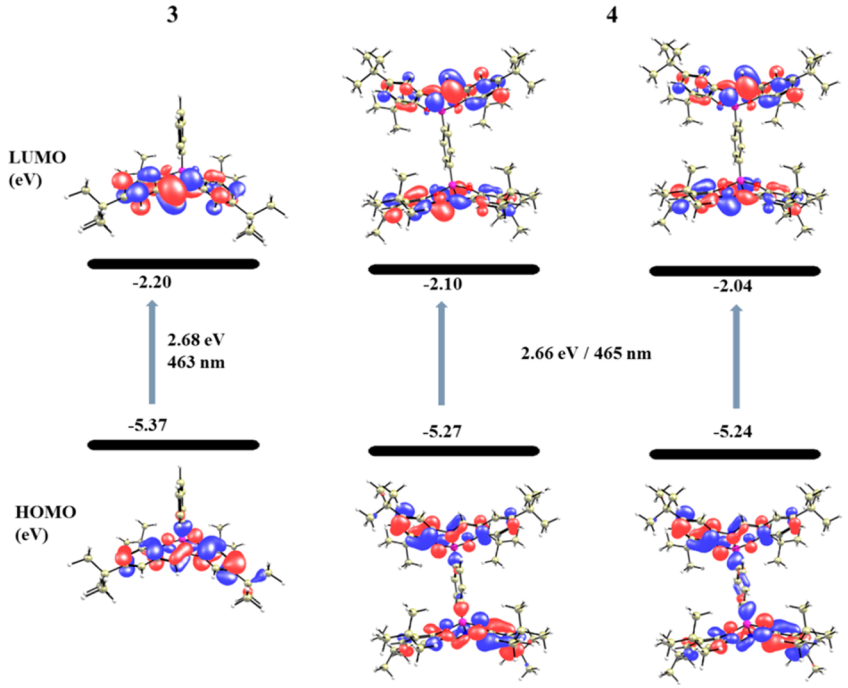

Figure 12. HOMO and LUMO molecular orbitals and their energies involved in the electronic transitions for complexes **3** and **4**.

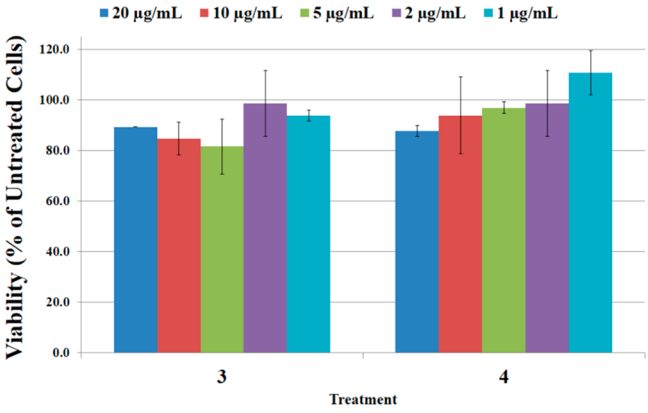

Figure 13. Effects of organoboron **3** and **4** on viability of A431 cells. Cell proliferation was determined by MTS after treatment with different concentrations of compounds **3** and **4** (20, 10, 5, 2, and 1 μg/mL) over 24 h.

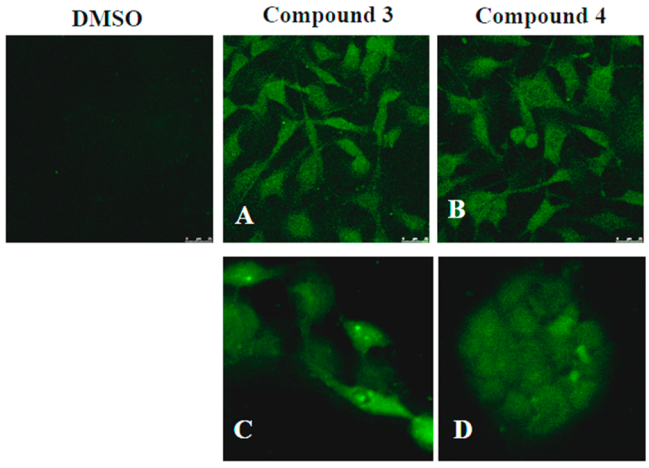

Figure 14. Staining of cells with organoboron compounds. Confocal microscopy of melanoma cells B16F10 (A, B) and A-431 (C, D) treated with 10 μg/mL of each compound for 2 h.

with an ATR accessory with a single-reflection ZnSe ATR crystal. UV spectra were obtained with a UV/vis spectrophotometer, and emission measurements were performed on a spectrofluorometer. ^{1}H, ^{13}C, and ^{11}B NMR spectra were recorded on a DPX 400. Chemical shifts (ppm) are relative to $(CH_3)_4Si$ for ^{1}H and ^{13}C. ^{11}B NMR spectra were referenced externally to $BF_3{\cdot}OEt_2$. Mass spectra were recorded on an API 2000 LC/MS/MS system.

4.2. Crystal Structure Determination. The crystals of **3** and **4** were covered with a layer of hydrocarbon oil that was selected and mounted with paratone-N oil on a cryo-loop and immediately placed in a low-temperature nitrogen stream at 100(2) K. The data for **3** and **4** were recorded on a diffractometer equipped with a graphite monochromator and a Mo Kα fine-focus sealed tube (λ = 0.71073 Å). The structure was solved by direct methods using SHELXS-97[36] and refined against F^2 on all data by full-matrix least-squares with SHELXL-97.[37] All of the software manipulations were done under the WIN-GX environment program set.[38] All heavier atoms were found by Fourier map difference and refined anisotropically. Some hydrogen atoms were found by Fourier map differences and refined isotropically. The remaining hydrogen atoms were geometrically modeled and are not refined. Crystallographic data for the structure reported in this paper have been deposited in the Cambridge Crystallographic Data Centre (CCDC 1518382 and 1518383).

4.3. Synthesis of (*E*)-2,4-Di-*tert*-butyl-6-((3,5-di-*tert*-butyl-2-hydroxybenzylidene)amino)phenol (2). A solution of 3,5-di-*tert*-butyl-6-hydroxyaniline (**1**) (0.66 g, 3 mmol) and 3,5-di-*tert*-butyl-2-hydroxybenzaldehyde (0.70 g, 3 mmol) in acetonitrile were heated under reflux for 48 h using a Dean–Stark apparatus for removal of water by azeotropic distillation. The reaction mixture was slowly cooled to room temperature, the solvent was evaporated, hexane was added, the precipitated solid was filtered and discarded, the liquor filtrate was concentrated, and acetonitrile was added. Solvent was allowed to evaporate slowly, and after 5 days yellow crystals were obtained that lost brightness over time, possibly due to crystallization with solvent. The compound was soluble in hexane to give 0.72 g. Yield: 54.9%. Mp: 104–105 °C. ^{1}H NMR (400 MHz, C_6D_6, 298 K): δ = 1.29 (s, 9H, *t* Bu-5), 1.31 (s, 9H, *t* Bu-10), 1.60 (s, 9H, *t* Bu-3), 1.63 (s, 9H, *t* Bu-12), 6.83 (d,1H, H4), 6.98 (d, 1H, H11), 7.43 (d, 1H, H9), 7.60 (d, 1H, H6), 8.13 (s, 1H, H7), 12.92 (s, 1H, OH). ^{13}C NMR (100 MHz, C_6D_6, 298 K): δ =

DOI: 10.1021/acs.joc.6b02802
J. Org. Chem. 2017, 82, 2375–2385

29.8 (CH_3, *t* Bu-3), 29.9 (CH_3, *t* Bu-12), 31.8 (CH_3, *t* Bu-5), 31.9 (CH_3, *t* Bu-10), 113.5 (C4), 122.9 (C6), 127.9 (C11), 128.1 (C9), 165.5 (C7). HETCOR [δ_H/δ_C]: 1.29/31.25 (CH_3, *t* Bu-5), 1.59/29.34 (CH_3, *t* Bu-3), 6.89/113.93 (H4/C4), 6.98/127.4 (H11/C11), 7.42/122.46 (H6/C6), 7.60/127.99 (H9/C9), 8.12/165.94 (H7/C7). COSY [δ_H/δ_H]: 7.43/6.82 (H6/H4), 7.60/6.98 (H9/H11). HRMS (APCI/TOF-Q) *m/z*: $[M + 1]^+$ calcd for $C_{29}H_{43}NO_2$ 438.3367, found 438.3368. IR ν (cm^{-1}): 3063 (OH), 1629 (C═N). UV−vis (THF): $\lambda_{abs/max}$, $\varepsilon_{max} \times 10^4$: 342 nm, 2.5 M^{-1} cm^{-1}. Fluorescence (THF): $\lambda_{Fluor/max}$ 507 nm.

4.4. Synthesis of 2,4,8,10-Tetra-*tert*-butyl-6-phenyldibenzo-[*d*,*h*][1,3,6,2]dioxazaboronine (3). A solution of **2** (0.219 g, 0.5 mmol) and phenylboronic acid (0.064 g, 0.52 mmol) in acetonitrile were heated under reflux for 48 h using a Dean−Stark apparatus for the removal of water by azeotropic distillation. The reaction mixture was slowly warmed to room temperature, and the solvent was concentrated and allowed to evaporate slowly at 12 h. Orange crystals were obtained. The compound was soluble in THF. Yield: 0.26 g (82.5%). Mp: 258−259 °C. ^{1}H NMR (400 MHz, THF-d_8, 298 K): δ = 1.32 (s, 9H, *t* Bu-5), 1.33 (s, 9H, *t* Bu-10), 1.45 (s, 9H, *t* Bu-3), 1.48 (s, 9H, *t* Bu-12), 6.98 (t, 1H, H-*p*), 7.26 (m, 2H, H-*o* and *m*), 7.32 (d, 1H, H11), 7.58 (d, 1H, H4), 7.51 (d, 1H, H6), 7.64 (d, 1H, H9), 8.78 (s, 1H, H7). ^{13}C NMR (100 MHz, THF-d_8, 298 K): δ = 29.9 (CH_3, *t* Bu-12), 30.2 (CH_3, *t* Bu-3), 31.9 (CH_3, *t* Bu-10), 32.2 (CH_3, *t* Bu-5), 35.1 (C_{quater}, *t* Bu-5), 35.6 (C_{quater}, *t* Bu-10), 35.7 (C_{quater}, *t* Bu-3), 36.3 (C_{quater}, *t* Bu-12), 110.9 (C6), 120.7 (C10), 126.1 (C11), 126.8 (C4), 127.8 (C-*p*), 132.3 (C-*o* and *m*), 133.0 (C9), 136.7 (C5), 140.1 (C12), 142.8 (C3), 142.6 (C1), 151.7 (C7), 155.1 (C2), 155.8 (C13). HETCOR [δ_H/δ_C]: 1.46/30 (CH_3, *t* Bu-3/C-*t* Bu-3), 1.32/31.91 (CH_3, *t* Bu-5/C-*t* Bu-5), 6.96/127.8 (H-*p*/C-*p*), 7.25/132.33 (H-*o* and *m*/C-*o* and *m*), 7.32/126.11 (H11/C11), 7.39/126.81 (H4/C4), 7.52/110.98 (H6/C6), 7.63/132.95 (H9/C9), 8.80/151.66 (H7/C7). COSY [δ_H/δ_H]: 7.26/6.97 (H-*o* and *m*/H-*p*). ^{11}B NMR (128 MHz, THF-d_8, 298 K): δ = 7.88 ppm. HRMS (APCI/TOF-Q) *m/z*: $[M + 1]^+$ calcd for $C_{35}H_{46}BNO_2$ 524.3694, found 524.3696. IR ν (cm^{-1}): 2957 (C−$H_{aromatic}$), 1627 (C═N). UV−vis (THF): $\lambda_{abs/max}$, $\varepsilon_{max} \times 10^4$ 455 nm, 1.4 M^{-1} cm^{-1}. Fluorescence (THF): $\lambda_{Fluo/max}$ 514 nm.

4.5. Synthesis of 1,4-Bis(2,4,8,10-tetra-*tert*-butyldibenzo-[*d*,*h*][1,3,6,2]dioxazaboronin-6-yl)benzene (4). A solution of **2** (0.44 g, 1 mmol), benzene-1,4-diboronic acid (0.083 g, 0.5 mmol), and acetic acid (0.5 mL) in acetonitrile was heated under reflux for 48 h using a Dean−Stark apparatus for the removal of water by azeotropic distillation. The reaction mixture was slowly warmed to room temperature; the precipitated solid was filtered and washed with hexane. The compound was partially soluble in acetone and THF, and it crystallized separately in acetone and a mixture of (THF/acetonitrile/acetone), obtaining yellow-orange crystals. Yield: 0.38 g (80.31%). Mp: 350−352 °C. ^{1}H NMR (400 MHz, THF-d_8, 298 K): δ = 1.20 (s, 18H, *t*-Bu-5), 1.23 (s, 18H, *t*-Bu-10), 1.32 (s, 18H, *t*-Bu-3), 1.36 (s, 18H, *t*-Bu-12, 6.98 (d, 4H, H-15), 7.06 (d, 2H, H11), 7.15 (d, 2H, H4), 7.18 (d, 2, H6), 7.46 (d, 2H, H9), 8.13 (d, 2H, H7). ^{13}C NMR (100 MHz, THF-d_6, 298 K): δ = 28.2 [(CH_3) *t*-Bu-12], 28.5 [(CH_3) *t*-Bu-3], 30.3 [(CH_3) *t*-Bu-10], 30.6 [(CH_3) *t*-Bu-5], 33.1 [(C_{quater}) *t*-Bu-5], 33.5 [(C_{quater}) *t*-Bu-10], 33.7 [(C_{quater}) *t*-Bu-3], 34.3 [(C_{quater}) *t*-Bu-12], 108.1 (C4), 124.1 (C11), 124.3 (C6), 129.3 (C15), 131.2 (C9), 147.1 (C7), 153.1 (C2), 153.8 (C13), 153.8 (C8). HETCOR [δ_H/δ_C]: 6.95/129.33 (H15/C15), 7.07/124.18 (H11/C11), 7.09/107.98 (H4/C4), 7.16/124.27 (H6/C6), 7.47/131.16 (H9/C9), 8.15/147.03 (H7/C7). COSY [δ_H/δ_H]: 7.46/7.06 (H9/H11). ^{11}B NMR (128 MHz, THF-d_8, 298 K): δ = 8.42 ppm. HRMS (APCI/TOF-Q) *m/z*: $[M + 1]^+$ calcd for $C_{64}H_{86}B_2N_2O_4$ 969.6846, found 969.6844. IR ν (cm^{-1}): 2955 (C−$H_{aromatic}$), 1617 (C═N). UV−vis (THF): $\lambda_{abs/max}$, $\varepsilon_{max} \times 10^4$ 455 nm, 2.1 $M^{-1}cm^{-1}$. Fluorescence (THF): $\lambda_{Fluor/max}$ 512 nm.

4.6. Absorbance, Emission, and Luminescence Quantum Yields. UV−vis absorption spectra were measured on a 365 spectrophotometer. Optical band gap (E_g) was determined from the intercept with the *X* axis of the tangent of the absorption spectrum drawn at absorbance of 0.1. The emission spectra have been recorded with a spectrofluorometer, by exciting 10 nm below the longer wavelength absorption band. Fluorescence quantum yields in solution were determined according to the procedure reported in literature[39] and using quinine sulfate in H_2SO_4 0.1 M as the standard. Three solutions with absorbance at the excitation wavelength lower than 0.1 were analyzed for each sample, and the quantum yield was averaged. The viscosity of the solvent mixture (methanol/glycerol) was determined using a Viscometer-ViscoLab 3000.

4.7. Cytotoxicity Assays in Cells and Cell Image. Human epidermoid carcinoma ATCC cell line A431 was employed to test the cytotoxic effects of compound **3** and **4**. A431 cells was maintained in Dulbecco's Modified Eagle Media (DMEM) with 4 mM L-glutamine and supplemented with 10% fetal bovine serum, 100 IU/mL of penicillin, and 100 g/mL of streptomycin. Culture of cell line was carried out at 37 °C in an incubator with 95% air and 5% CO_2 atmosphere. Cytotoxicity of compounds **3** and **4** was tested against this cell line at 1, 2, 5, 10, and 20 μg/mL. Tumor cells were seeded in 24-well tissue culture plates with 5×10^4 cells/well, and 24 h after platting they were supplemented by triplicate with compound s**3** and **4**. All dilutions were prepared with fresh culture media, and plates were incubated for 5 days. Cells in plates were washed with PBS pH = 7.4 to remove death cells. Surviving cells were measured by the MTS method [3-(4,5-dimethylthiazol-2-yl)-5-(3-carboxymethoxyphenyl)-2-(4-sulfophenyl)-2*H*-tetrazolium] and related to the mock cell population by measuring absorbance at 590 nm to establish cell viability with previous microscopic analysis for morphological changes exploration in cells.

B16F10 murine melanoma cells were seeded in 12-well plates on polylysine-coated sterile coverslips at a density of 1×10^5 cells per well in 1 mL of DMEM/F12 media supplemented with 10% fetal bovine serum and maintained at 37 °C in a controlled humid atmosphere of 5% CO_2 and 95% air. Twenty-four hours later, the medium was renewed and cells were exposed to the compounds at a concentration of 10 μg/mL (6.5 ppm) for 2 h. Untreated cells or treated with DMSO were used as controls. Supernatants were removed, and coverslips were washed once with 1 mL of PBS, mounted on microscope slips using Vectashield, and imaged using confocal laser microscopy. Samples were excited at 458 nm, and the fluorescence emission was measured at 478−612 nm for compounds **3** and **4**.

4.8. Computational Details. All calculations were performed using the GAUSSIAN 09 software package.[40] The geometry of structures **3** and **4** was fully optimized with the B3LYP l/6-31G(d,p) method.[41] The minima were characterized by calculating their vibrational modes at the same level of theory. In order to know the rotation energy of the phenyl group and one of the ligands, the bonds involved for that rotation were rotated by 30−180° or 360°, depending on the case. Results were visualized using the Chemcraft program v1.7.

■ ASSOCIATED CONTENT

Supporting Information

TThe Supporting Information is available free of charge on the ACS Publications website at DOI: 10.1021/acs.joc.6b02802.

X-ray crystallographic data for **3** and **4** (CIF)
Tables of crystallographic refinement parameters and geometric features for **3** and **4** (PDF)
Spectra for compounds **2**−**4** and crystal data for compounds **3** and **4** (PDF)

■ AUTHOR INFORMATION

Corresponding Author

*E-mail: victor.jimenezpr@uanl.edu.mx.

ORCID

H. V. Rasika Dias: 0000-0002-2362-1331
Víctor M. Jiménez-Pérez: 0000-0003-4306-2482

Notes

The authors declare no competing financial interest.

■ ACKNOWLEDGMENTS

This research was financially supported by CONACYT (Grant No. 240011). M.I.-R. thanks CONACYT for a scholarship (No.

DOI: 10.1021/acs.joc.6b02802
J. Org. Chem. 2017, 82, 2375−2385

227695). We thank the Laboratory of Immunology and Virology of FCB-UANL for the bioimaging cells. H.V.R.D acknowledges financial support received by the Robert A. Welch Foundation (Grant Y-1289).

DEDICATION

This work is dedicated to Prof. Cassandra L. Fraser as recognition of her scientific contribution on fluorescent materials.

REFERENCES

(1) Kuimova, M. K. *Phys. Chem. Chem. Phys.* **2012**, *14*, 12671−12686.
(2) Goh, W. L.; Lee, M. Y.; Joseph, T. L.; Quah, S. T.; Brown, C. J.; Verma, C.; Brenner, S.; Ghadessy, F. J.; Teo, Y. N. *J. Am. Chem. Soc.* **2014**, *136*, 6159−6162.
(3) (a) Loutfy, R. O.; Arnold, B. A. *J. Phys. Chem.* **1982**, *86*, 4205−4211. (b) Benjelloun, A.; Brembilla, A.; Lochon, P.; Adibnejad, M.; Viriot, M. L.; Carré, M. C. *Polymer* **1996**, *37*, 879−883.
(4) (a) Luka, S. *J. Am. Chem. Soc.* **1984**, *106*, 4386−4392. (b) Haidekker, M.; Brady, T.; Wen, K.; Okada, C.; Stevens, H.; Snell, J.; Frangos, J.; Theodorakis, E. *Bioorg. Med. Chem.* **2002**, *10*, 3627−4154. (c) Levitt, J. A.; Kuimova, M. K.; Yahioglu, G.; Chung, P. H.; Suhling, K.; Phillips, D. *J. Phys. Chem. C* **2009**, *113*, 11634−11642.
(5) (a) Haidekker, M. A.; Theodorakis, E. A. *Org. Biomol. Chem.* **2007**, *5*, 1669−1678. (b) Kuimova, M. K.; Botchway, S. W.; Parker, A. W.; Balaz, M.; Collins, H. A.; Anderson, H. L.; Suhling, K.; Ogilby, P. R. *Nat. Chem.* **2009**, *1*, 69−73. (c) Kuimova, M. K.; Yahioglu, G.; Levitt, J. A.; Suhling, K. *J. Am. Chem. Soc.* **2008**, *130*, 6672−6673. (d) Hungerford, G.; Allison, A.; McLoskey, D.; Kuimova, M. K.; Yahioglu, G.; Suhling, K. *J. Phys. Chem. B* **2009**, *113*, 12067−12074. (e) Peng, X.; Yang, Z.; Wang, J.; Fan, J.; He, Y.; Song, F.; Wang, B.; Sun, S.; Qu, J.; Qi, J.; Yan, M. *J. Am. Chem. Soc.* **2011**, *133*, 6626−6635.
(6) Tsai, A. G.; Friesenecker, B.; McCarthy, M.; Sakai, H.; Intaglietta, M. *Am. J. Physiol.* **1998**, *275*, H2170−H2180.
(7) (a) Alamiry, A. H.; Benniston, A. C.; Copley, G.; Elliott, K. J.; Harriman, A.; Stewart, B.; Zhi, Y.-G. *Chem. Mater.* **2008**, *20*, 4024−4032. (b) Li, J.; Zhang, Y.; Zhang, H.; Xuan, X.; Xie, M.; Xia, S.; Qu, G.; Guo, H. *Anal. Chem.* **2016**, *88*, 5554−5560. (c) Pal, S.; Chakraborty, H.; Bandari, S.; Yahioglue, G.; Suhling, K.; Chattopadhyay, A. *Chem. Phys. Lipids* **2016**, *196*, 69−75. (d) Xochitiotzi-Flores, E.; Jiménez Sánchez, A.; García Ortega, H.; Sánchez Puig, N.; Romero Ávila, M.; Santillán, R.; Farfán, N. *New J. Chem.* **2016**, *40*, 4500−4512. (e) Zhou, Y.; Chen, Y.-Z.; Cao, J.-H.; Yang, Q. Z.; Wu, L. Z.; Tung, C. H.; Wu, D. Y. *Dyes Pigm.* **2015**, *112*, 162−169. (f) Kim, E.; Felouat, A.; Zaborova, E.; Ribierre, J.; Wu, W.; Senatore, S.; Matthews, C.; Lenne, P. F.; Baffert, C.; Karapetyan, A.; Giorgi, M.; Jacquemin, D.; Vargas, M. P.; Guennic, B. L.; Fages, F.; D'Aléo, A. *Org. Biomol. Chem.* **2016**, *14*, 1311−1324.
(8) Alamiry, A. H.; Benniston, A. C.; Copley, G.; Elliott, V.; Harriman, A.; Stewart, B.; Zhi, Y.-G. *Chem. Mater.* **2008**, *20*, 4024−4032.
(9) Wang, D.; Miyamoto, R.; Shiraishi, Y.; Hirai, T. *Langmuir* **2009**, *25*, 13176−13182.
(10) Kuimova, M. K.; Yahioglu, G.; Levitt, J. A.; Suhling, K. *J. Am. Chem. Soc.* **2008**, *130*, 6672−6673.
(11) Karpenko, I. A.; Niko, Y.; Yakubovskyi, P.; Gerasov, A. O.; Bonnet, D.; Kovtun, Y. P.; Klymchenko, A. S. *J. Mater. Chem. C* **2016**, *4*, 3002−3009.
(12) (a) Jing, X.; Yu, F.; Chen, L. *Chem. Commun.* **2014**, *50*, 14253−14256. (b) Jiao, L.; Wu, Y.; Wang, S.; Hu, Y.; Zhang, P.; Yu, C.; Cong, K.; Meng, Q.; Hao, E.; Vicente, M. G. H. *J. Org. Chem.* **2014**, *79*, 1830−1835.
(13) (a) Kim, T.; Park, J.; Park, S.; Choi, Y.; Kim, Y. *Chem. Commun.* **2011**, *47*, 12640−12642. (b) Bernhard, Y.; Winckler, P.; Chassagnon, R.; Richard, P.; Gigot, E.; Perrier Cornet, J.; Decreau, R. A. *Chem. Commun.* **2014**, *50*, 13975−13978.
(14) (a) Wang, X.-d.; Song, X.-h.; He, C.-y.; Yang, C. J.; Chen, G.; Chen, X. *Anal. Chem.* **2011**, *83*, 2434−2437. (b) Huang, J.; Peng, A.; Fu, H.; Ma, Y.; Zhai, T.; Yao, J. *J. Phys. Chem. A* **2006**, *110*, 9079−9084.
(15) (a) Day, J. H. *Chem. Rev.* **1963**, *63*, 65. (b) Day, J. H. *Chem. Rev.* **1968**, *68*, 649−657.
(16) (a) Pang, J.; Marcotte, E. J. P.; Seward, C.; Brown, R. S.; Wang, S. *Angew. Chem., Int. Ed.* **2001**, *40*, 4042−4045. (b) Keefe, M.; Benkstein, K. D.; Hupp, J. T. *Coord. Chem. Rev.* **2000**, *205*, 201−228. (c) Fernandez-Moreira, V.; Thorp-Greenwood, F. L.; Coogan, M. P. *Chem. Commun.* **2010**, *46*, 186−202. (d) McLaurin, E. J.; Vlaskin, V. A.; Gamelin, D. R. *J. Am. Chem. Soc.* **2011**, *133*, 14978−14980. (e) Cui, Y.; Xu, H.; Yue, Y.; Guo, Z.; Yu, J.; Chen, Z.; Gao, J.; Yang, Y.; Qian, G.; Chen, B. *J. Am. Chem. Soc.* **2012**, *134*, 3979−3982. (f) Uchiyama, S.; Kawai, N.; de Silva, A. P.; Iwai, K. *J. Am. Chem. Soc.* **2004**, *126*, 3032−3033.
(17) Dias, H. V. R.; Diyabalanage, H. V. K.; Eldabaja, M. G.; Elbjeirami, O.; Rawashdeh-Omary, M. A.; Omary, M. A. *J. Am. Chem. Soc.* **2005**, *127*, 7489−7501.
(18) Benito, Q.; Le Goff, F.; Nocton, G.; Fargues, A.; Garcia, A.; Berhault, A.; Kahlal, S.; Saillard, J. Y.; Martineau, C.; Trebosc, J.; Gacoin, T.; Boilot, J.-P.; Perruchas, S. *Inorg. Chem.* **2015**, *54*, 4483−4494.
(19) Chen, K.; Catalano, V. J. *Eur. J. Inorg. Chem.* **2015**, *2015*, 5254−5261.
(20) Liu, X.; Li, S.; Feng, J.; Li, Y.; Yang, G. *Chem. Commun.* **2014**, *50*, 2778−2780.
(21) Chan-Navarro, R.; Jiménez-Pérez, V.; Muñoz Flores, B. M.; Dias, R.; Moggio, I.; Arias, E.; Ramos Ortíz, G.; Santillán, R.; García, C.; Ochoa, M. E.; Yousufuddin, M.; Waksman, N. *Dyes Pigm.* **2013**, *99*, 1036−1043.
(22) (a) Farfán, N.; Mancilla, T.; Uribe, G.; Carrillo, L.; Joseph-Nathan, P.; Contreras, R. *J. Organomet. Chem.* **1990**, *381*, 1−13. (b) Lamère, J. F.; Lacroix, P. G.; Farfán, N.; Rivera, J. M.; Santillan, R.; Nakatani, K. *J. Mater. Chem.* **2006**, *16*, 2913−2920.
(23) (a) Barba, V.; Vazquez, J.; López, F.; Santillán, R.; Farfán, N. *J. Organomet. Chem.* **2005**, *690*, 2351−2357. (b) Noeth, H.; Wrackmeyer, B. *Nuclear Magnetic Resonance Spectroscopy of Boron Compounds*; Springer-Verlag: New York, 1978.
(24) Muñoz, B.; Santillán, R.; Rodríguez, M.; Méndez, J.; Romero, M.; Farfán, N.; Lacroix, P.; Nakatani, K.; Ramos, G.; Maldonado, J. *J. Organomet. Chem.* **2008**, *693*, 1321−1334.
(25) Barba, V.; Cuahutle, D.; Santillan, R.; Farfán, N. *Can. J. Chem.* **2001**, *79*, 1229−1237.
(26) Kaiser, F.; White, M.; Hutton, C. A. *J. Am. Chem. Soc.* **2008**, *130*, 16450−16451.
(27) Hopfl, H. *J. Organomet. Chem.* **1999**, *581*, 129−137.
(28) Kottas, G. S.; Clarke, L. I.; Horinek, D.; Michl, J. *Chem. Rev.* **2005**, *105*, 1281−1376.
(29) Haidekker, M.; Brady, T.; Lichlyter, D.; Theodorakis, E. *Bioorg. Chem.* **2005**, *33*, 415−489.
(30) (a) Yusop, M.; Unciti Broceta, A.; Bradley, M. *Bioorg. Med. Chem. Lett.* **2012**, *22*, 5780−5783. (b) Kuimova, K.; Yahioglu, G.; Levitt, J. A.; Suhling, K. *J. Am. Chem. Soc.* **2008**, *130*, 6672−6673. (c) Karpenko, A.; Niko, Y.; Yakubovskyi, P.; Gerasov, A. O.; Bonnet, D.; Kovtun, Y. P.; Klymchenko, A. S. *J. Mater. Chem. C* **2016**, *4*, 3002−3009.
(31) Chen, Z.; Liang, J.; Nie, Y.; Xu, X.; Yu, G.-A.; Yin, J.; Liu, H. *Dalton Trans.* **2015**, *44*, 17473−17477.
(32) Seki, T.; Takamatsu, Y.; Ito, H. *J. Am. Chem. Soc.* **2016**, *138*, 6252−6260.
(33) (a) Sancho-García, J. C.; Cornil, J. *J. Chem. Phys.* **2004**, *121*, 3096−3101. (b) Wong, B. M.; Raman, S. J. *J. Comput. Chem.* **2007**, *28*, 759−766.
(34) (a) Santos, M. F.; Rosa, J. N.; Candeias, N. R.; Carvalho, C. P.; Matos, I.; Ventura, E.; Florindo, F.; Silva, C.; Pischel, U.; Gois, M. P. *Chem. - Eur. J.* **2016**, *22*, 1631−1637. (b) Zhou, Y.; Chen, Y.-Z.; Cao, J.-H.; Yang, Q.-Z.; Wu, L.-Z.; Tung, C.-H.; Wu, D.-Y. *Dyes Pigm.* **2015**, *112*, 162−169.
(35) Jiménez Pérez, V. M.; Camacho Camacho, C.; Güizado Rodríguez, M.; Noeth, H.; Contreras, R. *J. Organomet. Chem.* **2000**, *614*−*615*, 283−293.
(36) Sheldrick, G. M. *Acta Crystallogr., Sect. A: Found. Crystallogr.* **1990**, *46*, 467−473.

DOI: 10.1021/acs.joc.6b02802
J. Org. Chem. 2017, 82, 2375−2385

(37) Sheldrick, G. M. *SHELX-97*; Universität Göttingen: Göttingen, 1997.
(38) Farrugia, L. J. *J. Appl. Crystallogr.* **1999**, *32*, 837−838.
(39) Williams, A. T. R.; Winfield, S. A.; Miller, J. N. *Analyst* **1983**, *108*, 1067−1071.
(40) Frisch, M. J.; Trucks, G. W.; Schlegel, H. B.; Scuseria, G. E.; Robb, M. A.; Cheeseman, J. R.; Scalmani, G.; Barone, V.; Mennucci, B.; Petersson, G. A.; Nakatsuji, H.; Caricato, M.; Li, X.; Hratchian, H. P.; Izmaylov, A. F.; Bloino, J.; Zheng, G.; Sonnenberg, J. L.; Hada, M.; Ehara, M.; Toyota, K.; Fukuda, R.; Hasegawa, J.; Ishida, M.; Nakajima, T.; Honda, Y.; Kitao, O.; Nakai, H.; Vreven, T.; Montgomery, J. A., Jr.; Peralta, J. E.; Ogliaro, F.; Bearpark, M.; Heyd, J. J.; Brothers, E.; Kudin, K. N.; Staroverov, V. N.; Kobayashi, R.; Normand, J.; Raghavachari, K.; Rendell, A.; Burant, J. C.; Iyengar, S. S.; Tomasi, J.; Cossi, M.; Rega, N.; Millam, M. J.; Klene, M.; Knox, J. E.; Cross, J. B.; Bakken, V.; Adamo, C.; Jaramillo, J.; Gomperts, R.; Stratmann, R. E.; Yazyev, O.; Austin, A. J.; Cammi, R.; Pomelli, C.; Ochterski, J. W.; Martin, R. L.; Morokuma, K.; Zakrzewski, V. G.; Voth, G. A.; Salvador, P.; Dannenberg, J. J.; Dapprich, S.; Daniels, A. D.; Farkas, Ö.; Foresman, J. B.; Ortiz, J. V.; Cioslowski, J.; Fox, D. J. *Gaussian 09*, revision B.01; Gaussian, Inc.: Wallingford CT, 2009.
(41) (a) Becke, A. D. *J. Chem. Phys.* **1993**, *98*, 5648−5652. (b) Petersson, G. A.; Al-Laham, M. A. *J. Chem. Phys.* **1991**, *94*, 6081−6090.

DOI: 10.1021/acs.joc.6b02802
J. Org. Chem. 2017, 82, 2375−2385